Four-Quadrant Propeller Modeling: A Low-Order Harmonic Approximation ⋆

Andreas J. Häusler * **Alessandro Saccon** ** **John Hauser** ***
António M. Pascoal *,**** **A. Pedro Aguiar** *,*****

* *Laboratory of Robotics and Systems in Engineering and Science (LARSyS), Instituto Superior Técnico (IST), University of Lisbon, Portugal (ahaeusler@isr.ist.utl.pt)*
** *Eindhoven University of Technology, The Netherlands (a.saccon@tue.nl)*
*** *University of Colorado at Boulder, USA (john.hauser@colorado.edu)*
**** *Adjunct Scientist, National Institute of Oceanography (NIO), Goa, India (antonio@isr.ist.utl.pt)*
***** *Faculty of Engineering of the University of Porto (FEUP), Porto, Portugal (pedro.aguiar@fe.up.pt)*

Abstract: We propose a four-quadrant propeller model suitable for energy-efficient motion planning of autonomous marine vehicles. The model can be used to capture the main features of experimental thrust and torque curves by using a small number of parameters. We explore the connection between the propeller thrust, torque, and efficiency curves and the lift and drag curves of the propeller blades.
The model originates from a well-known four-quadrant model, based on a sinusoidal approximation of the propeller curves, nontrivially modified in this paper to account for the typical drop off in the efficiency curve in correspondence to thrust inversion. Connections with the standard first-quadrant open-water model are drawn.

Keywords: Propeller Modeling, Four-Quadrant Propeller Model, Open-Water Propeller Model, Open-Water Efficiency, Harmonic Approximation.

1. INTRODUCTION

Despite being available for almost half a century, four-quadrant propeller models are not widely used in the marine robotics community. The method of choice in the vast majority of publications continues to be the *open-water model*

$$T = \rho d^4 k_{\mathrm{T}}(J_{\mathrm{o}}) n^2 \tag{1}$$

$$Q = \rho d^5 k_{\mathrm{Q}}(J_{\mathrm{o}}) n^2 \tag{2}$$

in which the propeller thrust T and torque Q are characterized by the (dimensionless) open-water coefficients $k_T(J_o)$ and $k_Q(J_o)$, respectively, where $J_o = v_a/nd$ is the advance ratio and n is the propeller rotational velocity, d the propeller diameter, v_a the vessel's advance speed, and ρ the water density.

The above model is adequate for the case of marine vehicles designed to keep a minimum speed with respect to the water and to maneuver using control surfaces. This is in striking contrast to the situation that arises during the operation of marine vehicles that are purely thruster propelled. In this case, the forces and torques required to maneuver the vehicle must necessarily be obtained by recruiting the common and differential modes of paired-up propellers. For example, a vehicle moving in the 2D horizontal plane will recruit the common and differential thrust $T_{\mathrm{c}} = \frac{1}{2}(T_{\mathrm{ps}} + T_{\mathrm{sb}})$ and $T_{\mathrm{d}} = \frac{1}{2}(T_{\mathrm{ps}} - T_{\mathrm{sb}})$, where T_{ps} and T_{sb} are the thrust generated by the starboard and port side propellers, respectively. Clearly, during station keeping or cruising maneuvers that require fast turnings, the thrusters will be required to operate in regions that are not covered by the first-quadrant model (1) and (2), which contemplates only the situation where both n and v_a are positive. As such, the model fails to describe other regions of operation (e.g. $n < 0$ and $v_a > 0$) and, in particular, the behavior caused by sign changes in the propeller speed n (0-crossing) that make the advance ratio J_0 go through infinity.

Thus, for small ocean vehicles, especially those steered by differential thrust from two or more propellers (and not by changing the deflection of a rudder), a different model should be used, since it is highly likely that the propellers will change their rotational direction for maneuvers that involve curved trajectories. The *four-quadrant model*, described in the seminal paper of van Lammeren et al. (1969), is valid for operations in all regions of motion (those regions are commonly referred to as ahead, crash-back, back, and crash-ahead in reference to the four quadrants of the advance angle β, as shown in Fig. 1). The coefficients of this model are given in terms of the advance angle β at the propeller blade (see Fig. 1 and the definition below), and experimental data are available in the form of a 20th order Fourier series for various (ducted) propellers and nozzles; see the original work of van Lammeren et al. (1969) as well as the Ph.D. thesis of Oosterveld (1970). An extensive discussion of the four-quadrant model in relation to control and thrust estimation is given in Pivano (2008).

In the four-quadrant model, the propeller thrust and torque are

$$T = \frac{1}{2}\rho c_{\mathrm{T}}(\beta)\left(v_{\mathrm{a}}^2 + v_{\mathrm{p}}^2\right)\pi R^2 \tag{3}$$

$$-Q = \frac{1}{2}\rho c_{\mathrm{Q}}(\beta)\left(v_{\mathrm{a}}^2 + v_{\mathrm{p}}^2\right)\pi R^2 d \tag{4}$$

⋆ Research supported in part by projects MORPH of the EU FP7 (grant agreement no. 288704) and CONAV of the FCT (contract number PTCD/EEA-CRO/113820/2009), and by the FCT Program PEst-OE/EEI/LA0009/2011.
The work of A. Häusler was supported with a Ph.D. scholarship of the FCT under grant number SFRH/BD/68941/2010.
The research results presented in this paper were partly obtained while A. Häusler was a visiting scholar at the University of Colorado at Boulder.

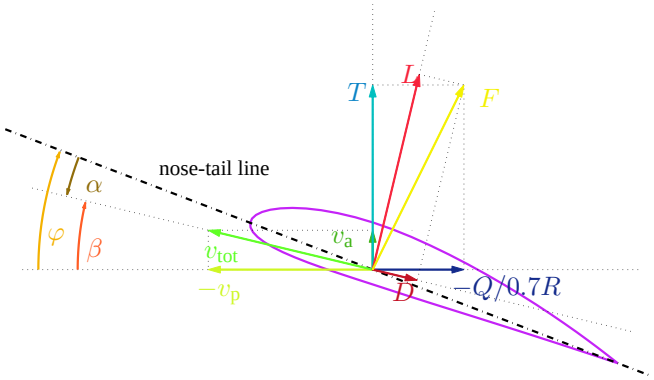

Fig. 1. Forces and velocities acting on a propeller blade. The propeller is assumed to be left-rotating for forward-thrust generation, i.e. the vehicle (and thus the propeller) is moving upwards in this picture, while the propeller to the left (i.e. into the page).

where R and $d = 2R$ are the propeller radius and diameter, respectively, v_a is the ambient water velocity, and v_p is the tangential velocity of the propeller at a distance of $0.7R$ from the propeller axis [1]. The propeller tangential velocity v_p is related to the propeller angular speed ω via

$$v_p = 0.7R\omega. \tag{5}$$

Because $\omega = 2\pi n$, the above equation can also be written as $v_p = 0.7d\pi n$. The minus sign appearing in front of Q in the left hand side of (4) ensures that moments and forces are consistent with the right-hand rule with the conventions depicted in Fig. 1. The thrust and torque coefficients c_T and c_Q are functions of the propeller blade advance angle β, classically defined in the literature as $\text{atan2}(v_a, v_p)$. Notice, however, that this definition is appropriate just for propellers that rotate *clockwise*. In this paper we are interested in an anticlockwise rotating propeller, as the one depicted in Fig. 1, and it is important at this point to explain the impact this has on the standard four-quadrant expressions that consider a clockwise rotating propeller. By convention, when n is positive, the propeller is rotating clockwise (seen from behind the vessel) and when n is negative, the propeller is rotating anticlockwise. From (5), remembering that $\omega = 2\pi n$, we see that the sign of n determines the sign of v_p, which in turn influences the value of β. In order to compute β in accordance with what is shown in Fig. 1, we thus have to define the advance angle β as

$$\beta = \pi - \text{atan2}(v_a, v_p).$$

The terms of the periodic functions $c_T(\beta)$ and $c_Q(\beta)$ are given as Fourier series in van Lammeren et al. (1969) and Oosterveld (1970) for ducted and ductless propellers, with various combinations of nozzles and pitch ratios. The data published are sufficiently vast to be of practical use for a large number of commercially available thrusters. This applies to the Seabotix HPDV 1507 thrusters with a type 37 Kort nozzle that are used in IST's MEDUSAS vehicles (Häusler et al., 2012) and are taken as a case study here.

The pitch angle of the Seabotix propellers is $\varphi = 23.2°$, and the pitch ratio p/d, with p being the (unknown) propeller pitch, can be computed as (Fig. 3.4 in Carlton, 2007)

$$\frac{p}{d} = \pi \tan\varphi \approx 1.3465 \tag{6}$$

[1] Rooted in blade geometry considerations (Carlton, 2007, Sec. 3.3), the four-quadrant model, by definition, describes the interaction of the propeller blade with the water at $0.7R$.

The closest pitch ratio value to (6) in Oosterveld (1970) is $p/d = 1.4$ for a Wageningen Ka 4-70 propeller running in a duct of the same shape as the Seabotix propellers, so we make use of the corresponding Fourier series in this paper.

Remark 1. A correction factor can be applied to achieve the bollard-pull conditions that Seabotix indicates for its HPDC 1507 thruster model in the following manner: from the manufacturer's specifications, the maximum propeller velocity can be obtained, which is sufficient to compute the values of thrust (3) and torque (4) at bollard-pull conditions (i.e. $v_a = 0.0\,\frac{\text{m}}{\text{s}}$) for the Wageningen Ka 4-70 propeller with $p/d = 1.4$, running in a Type 37 Kort nozzle (Oosterveld, 1970). These values can be compared with the manufacturer data of maximum continuous thrust and torque at bollard-pull conditions achievable with the Seabotix thrusters, which leads to a multiplicative correction factor for c_T and c_Q. For clarity of the presentation, the correction factor is not accounted for in this work; however, our trajectory planning work (see e.g. Häusler et al. (2013)) does indeed implement these correction factors. □

Remark 2. According to (Carlton, 2007, Sec. 3.3), the Wageningen propeller series were designed using the face pitch line to measure the pitch angle, and not, as assumed here, the nose-tail line of the blade. The difference can be assumed to be on the order of $\pm 5°$. □

2. THE SIMPLIFIED FOUR-QUADRANT MODEL BY HEALEY ET AL.

The key motivation for the work reported here stems from our interest in developing algorithms for the computation of energy-optimal trajectories for multiple vehicles acting in cooperation, with due account for full vehicle and actuator dynamics—see Häusler et al. (2013) and the references therein. In the case of purely propelled vehicles, this requires the use of a complete propulsion model (consisting of a model of the propeller plus the electric motor ensemble) allowing for the computation of the actual energy that is spent for vehicle motion.

The optimizer at the core of our trajectory planning framework is a Newton descent method that makes use of a twice continuously differentiable ($\mathcal{C}^2$) cost functional (Hauser, 2002), which requires that *both* the cost and dynamics be $\mathcal{C}^2$. If one extends, by symmetry, the first quadrant open-water model to four-quadrant operation, the result is not even continuous everywhere and is thus not appropriate for use in derivative based optimization. Direct use of the Wageningen series four-quadrant model has also proved to be problematic, wherein the optimization is not able to switch to second order descent, indicating that the dynamically constrained problem either does not possess a minimizing trajectory or that the second order approximation at the minimizer is not positive definite in an appropriate sense. We suspect that the roughness or non-monotonicity of the corresponding thrust and torque curves, shown in the leftmost plots of Fig. 2, may play a role.

Idealized curves such as those in (Fossen, 1994, Fig. 4.3) are appealing for use in optimization, and the approximation of the four-quadrant model published by Healey et al. (1995), and used in the work of Whitcomb and coworkers (Whitcomb and Yoerger, 1999; Bachmayer et al., 2000) provides such an idealized model. Healey et al. suggest a model (called the "**H**-model" from here on) where the lift and drag coefficients of the propeller are described by

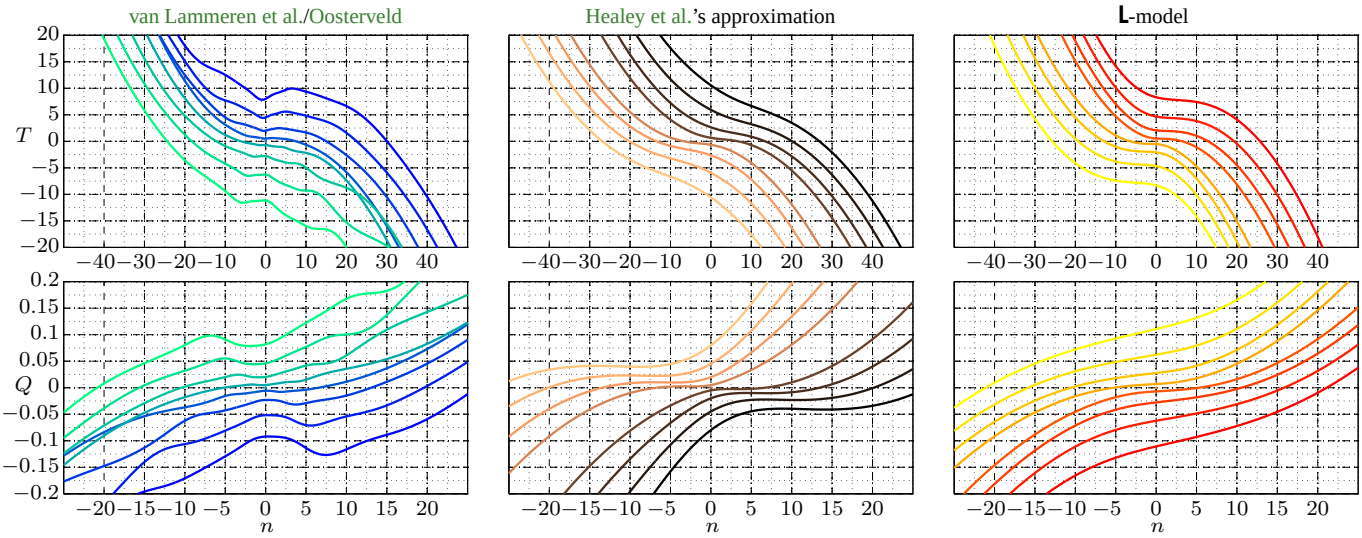

Fig. 2. Level curves of four-quadrant thrust T and torque Q as obtained from the original data published by Oosterveld, the approximation of Healey et al., and the **L**-model. The plots show thrust and torque for different values of the advance velocity ($v_\mathrm{a} \in [-2,2]\,\frac{\mathrm{m}}{\mathrm{s}}$ with a step size of $0.5\,\frac{\mathrm{m}}{\mathrm{s}}$; darker colors are negative, lighter colors are positive v_a).

$$c_\mathrm{L}^{\mathbf{H}}(\alpha) = c_\mathrm{L}^{\max} \sin 2\alpha \tag{7}$$
$$c_\mathrm{D}^{\mathbf{H}}(\alpha) = c_\mathrm{D}^{\max} (1 - \cos 2\alpha)/2 \tag{8}$$

where $\alpha = \phi - \beta$ is the angle of attack of the propeller blade (cf. Fig. 1). In (8), we have introduced a factor of $1/2$, not present in the original, so that the maximum drag coefficient is indeed $c_\mathrm{D}^{\max}$.

The propeller thrust T and torque Q are related to propeller lift L and drag D through a rotation by the advance angle β, namely

$$\begin{bmatrix} L \\ D \end{bmatrix} = \begin{bmatrix} \cos\beta & -\sin\beta \\ -\sin\beta & -\cos\beta \end{bmatrix} \begin{bmatrix} T \\ -Q/(0.7R) \end{bmatrix}. \tag{9}$$

The above relationship can be inferred by geometric considerations from Fig. 1. It is assumed, in accordance with the four-quadrant model detailed in the introduction, that the propeller torque Q is related to the tangential force acting on the propeller blade through a lever arm with length $0.7R$.

Substituting the expressions for T and Q given by (3) and (4) in (9), we obtain

$$L = \frac{1}{2}\rho\big(v_\mathrm{a}^2 + v_\mathrm{p}^2\big) R^2 \Big(\quad c_\mathrm{T}(\beta)\cos\beta + \frac{d}{0.7R} c_\mathrm{Q}(\beta)\sin\beta \Big),$$
$$D = \frac{1}{2}\rho\big(v_\mathrm{a}^2 + v_\mathrm{p}^2\big) R^2 \big(-c_\mathrm{T}(\beta)\sin\beta + \frac{d}{0.7R} c_\mathrm{Q}(\beta)\sin\beta \big).$$

Since $\beta = \varphi - \alpha$, we can determine $c_\mathrm{L}^{\max}$ and $c_\mathrm{D}^{\max}$ by rotating the thrust and torque coefficients into the lift-and-drag frame, that is, obtaining

$$c_\mathrm{L}^{\mathbf{O}}(\alpha) = c_\mathrm{T}^{\mathbf{O}}(\varphi-\alpha)\cos(\varphi-\alpha) - \frac{2}{0.7}\big(-c_\mathrm{Q}^{\mathbf{O}}(\varphi-\alpha)\big)\sin(\varphi-\alpha),$$
$$c_\mathrm{D}^{\mathbf{O}}(\alpha) = -c_\mathrm{T}^{\mathbf{O}}(\varphi-\alpha)\sin(\varphi-\alpha) - \frac{2}{0.7}\big(-c_\mathrm{Q}^{\mathbf{O}}(\varphi-\alpha)\big)\cos(\varphi-\alpha),$$

and finding the maxima of these expressions. The result is shown as dashed lines in Fig. 4. We call this the "**O**-model" in reference to Oosterveld (1970). The lift and drag coefficients obtained in this manner can now be rotated back into the thrust and torque frame, yielding

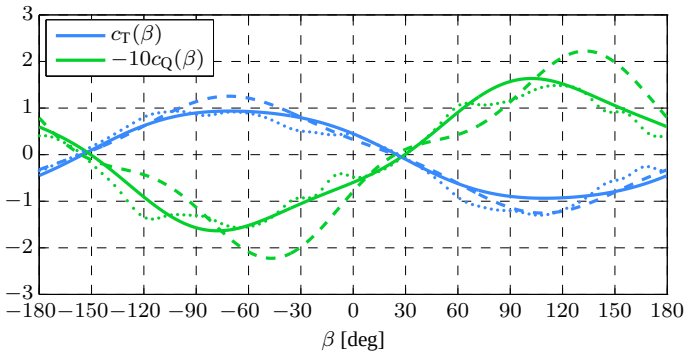

Fig. 3. Four-quadrant thrust and torque coefficients, scaled for MEDUSAS. The figure shows Oosterveld's original Fourier series (dotted), the simplification of Healey et al. (rotated from the lift-and-drag frame into the thrust-and-torque frame; dashed), and our own sinusoidal model (solid).

$$c_\mathrm{T}^{\mathbf{H}}(\beta) = c_\mathrm{L}^{\mathbf{H}}(\beta)\cos\beta - c_\mathrm{D}^{\mathbf{H}}(\beta)\sin\beta$$
$$c_\mathrm{Q}^{\mathbf{H}}(\beta) = -\frac{0.7}{2}\big(-c_\mathrm{L}^{\mathbf{H}}(\beta)\sin\beta - c_\mathrm{D}^{\mathbf{H}}(\beta)\cos\beta\big)$$

which results in the coefficient curves shown in Fig. 3.

Remark 3. Clearly, the rotations between the lift-and-drag and the thrust-and-torque frame ignore results from the vorticity of the propeller, as well as the induced velocity v_i at the propeller blade (Breslin and Andersen, 1994). In contrast to the results presented here, the rotations should be done about the *induced* advance angle β_i and the coefficients then be obtained through integration along the blade, using the propeller radius (Glauert, 1947). It remains an open question how significant the resulting higher accuracy of the model would be; for now, we ignore these considerations in favor of simplicity of the model. □

3. THE **L**-MODEL

Closer examination of the **H**-model, i.e. the approximation of the original four-quadrant data by coefficients obtained by rotation of sinusoidal lift and drag curves into the thrust-and-torque frame, may fail to capture some physical constraints, resulting from the fact that the lift and drag curves (Fig. 4, dashed lines) are somewhat "synchronized": they go through the origin at exactly the same angle of attack ($\alpha = 0°$ and $\alpha = -180°$). This propagates into the thrust and torque coefficient

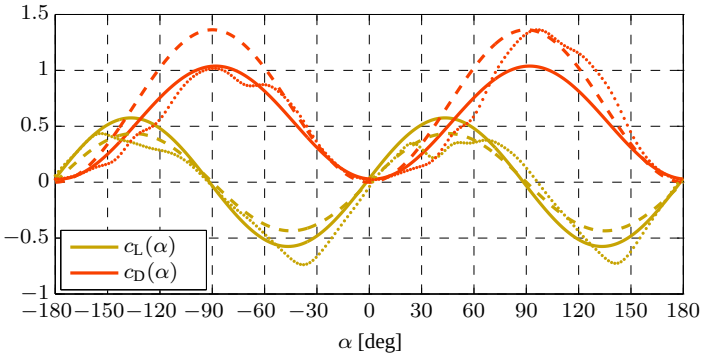

Fig. 4. Lift and drag coefficients. The figure shows the original Fourier series data (the **O**-model, dotted), the **H**-model (dashed), and the **L**-model (solid).

curves (Fig. 3, dashed lines): both coefficients are zero for an advance angle of $\beta = 24.02°$ and $\beta = -155.98°$, respectively.

Since both the thrust and torque contain the coefficients $c_T(\beta)$ and $c_Q(\beta)$ in a multiplicative form (see (3) and (4)), this means that for the original **H**-model, thrust T and torque Q go through 0 at the same advance angle. Physics, however, suggest that for a propeller in general, but especially one that has approximately the pitch ratio of our Seabotix propellers (6), the thrust must go to 0 slightly *before* the torque reaches 0—see, for instance, (Fossen, 2002, Fig. 12.2), van Lammeren et al. (1969), or (Oosterveld, 1970, Fig. 37), and the explanation of our results in Sec. 4.1. Similarly, drag can be expected to attain its minimum for a slightly positive lift—see the important remarks in (Anderson, 1999, p. 132), illustrated by the drag polar diagrams in (Abbott and von Doenhoff, 1959, Chapter 7). In addition, the minimum of $c_D(\alpha)$ should be non-negative (Sheldal and Kilmee, 1981) because of a *residual drag* component that is missing in the **H**-model.

The consequences of the assumptions underlying the **H**-model can be best examined by looking at the characteristic *open-water* (i.e. first-quadrant model) *efficiency* curve of the **H**-model in comparison to what is suggested in the marine engineering literature. The efficiency can be obtained for the four-quadrant model in the following fashion: first, following the exposition in (Smogeli, 2006, Sec. 2.1.2) or (Clayton and Bishop, 1982, Sec. 7.7.1), the first-quadrant thrust and torque coefficients $k_T(J_o)$ and $k_Q(J_o)$ are related to the four-quadrant coefficients $c_T(\beta)$ and $c_Q(\beta)$ as

$$k_T(J_o) = \frac{\pi}{8} c_T(\beta)\left(J_o^2 + 0.7^2\pi^2\right)$$
$$k_Q(J_o) = \frac{\pi}{8} c_Q(\beta)\left(J_o^2 + 0.7^2\pi^2\right)$$

where the argument of k_T and k_Q, the open-water advance ratio J_o, is defined for left-rotating propellers as

$$J_o = -0.7R\tan(\pi - \beta) = 0.7R\tan\beta \tag{10}$$

The open-water propeller efficiency can then be computed as in (Fossen, 2002, Sec. 12.2):

$$\eta = \frac{J_o}{2\pi}\frac{k_T}{k_Q}$$

The expected efficiency curve, also verified by the Oosterveld data (leftmost plot in Fig. 5), rises from the origin in a "close to linear" manner to a peak efficiency $\eta < 1.0$, before falling back to 0, which marks the point where the thrust coefficient c_T changes its sign for non-zero advance velocity v_a. Instead of falling back to 0, the efficiency curve from Healey et al.'s approximation of the original four-quadrant model goes *through* $\eta = 1.0$ and continues growing without exhibiting a local maximum.

For the aforementioned reasons, we suggest the following modification of the **H**-model:

Definition 4. The **L**-model of a propeller is defined through the relations

$$c_L^{\mathbf{L}}(\alpha) = c_L^{\max}\sin 2(\alpha - o_L) \tag{11}$$
$$c_D^{\mathbf{L}}(\alpha) = \left(c_D^{\max} - c_D^{\min}\right)\left(1 - \cos 2(\alpha - o_D)\right)/2 + c_D^{\min} \tag{12}$$

where (11) and (12) are intended to replace (7) and (8), respectively. □

We determined the five parameters ($c_L^{\max}$, $c_D^{\min}$, $c_D^{\max}$, o_L, o_D) in the **L**-model (11), (12) to obtain a low order approximation of the **O**-model by solving a nonlinear least squares problem that seeks to capture characteristics of first quadrant open-water efficiency (Fig. 6) while fitting the $c_T(\beta)$ and $c_Q(\beta)$ curves in the primary operating region $0° \le \beta \le 50°$ (Fig. 3). We have also enforced a monotonicity constraint on the level curves of the produced thrust [2] (Fig. 2, rightmost plot). Numerical values of the parameters were found to be $o_L = -1.6157°$, $o_D = 1.9309°$, $c_D^{\min} = 0.0273$, $c_L^{\max} = 0.5749$, and $c_D^{\max} = 1.0383$. With the obtained values of $o_L \neq o_D$, we find that the minimum drag is indeed obtained at a slight positive lift which is in line with what is common for real airfoils (Anderson, 1999). With the inclusion of three additional parameters, the **L**-model appears to be capable of capturing a number of efficiency related features (see Sec. 4.2) that the **H**-model does not exhibit.

The **L**-model, as Fig. 4 reveals (solid and dashed lines), is a minor modification in terms of the lift and drag coefficients, yet it prevents both from crossing 0 at the same angle of attack. The resulting thrust and torque coefficients (Fig. 3, again obtained by rotation) achieve the desired shape of the efficiency curve (Fig. 5) in the first quadrant.

Remark 5. Due to the (imposed) symmetry between the different modes of operation, the **H**-model and **L**-model do not show the double cover of the J_o axis as the **O**-model does (see Fig. 5). In these models, the propeller exhibits the same characteristics in ahead and crash ahead (i.e. $\beta \in (0, \pi)$ as it does in back and crash back mode (i.e. $\beta \in (\pi, 2\pi)$). Since Oosterveld's model was obtained from experimental data where the propellers are designed for the purpose of forward propulsion in conjunction with non-backward-forward-symmetric flow-accelerating nozzles, the coefficients show different characteristic curves for $\beta \in (0, \pi)$ and $\beta \in (\pi, 2\pi)$. Viewed as Fourier series, our **L**-model results in curves for c_L and c_D that only contain constant and first harmonic (which leads, by rotation, to the presence of first and third harmonics in our c_T and c_Q curves). Clearly, a Fourier series model that includes only a single frequency (in addition to a constant term) is incapable of capturing the aforementioned asymmetric behavior. □

4. EFFICIENCY ANALYSIS

On four quadrants, the propeller efficiency η is defined as the ratio between the available power for vehicle propulsion and the rotational power provided by the electric motor, namely

$$\eta = \frac{Tv_a}{Q\omega}. \tag{13}$$

Our goal is to obtain a low complexity model that reproduces in an accurate way the energy flow in the four possible quadrants

[2] Interestingly, monotonicity of $T(n)$ turned out not to be an active constraint at the minimizing solution to the $\mathcal{L}_2$-fit of the **L**-model.

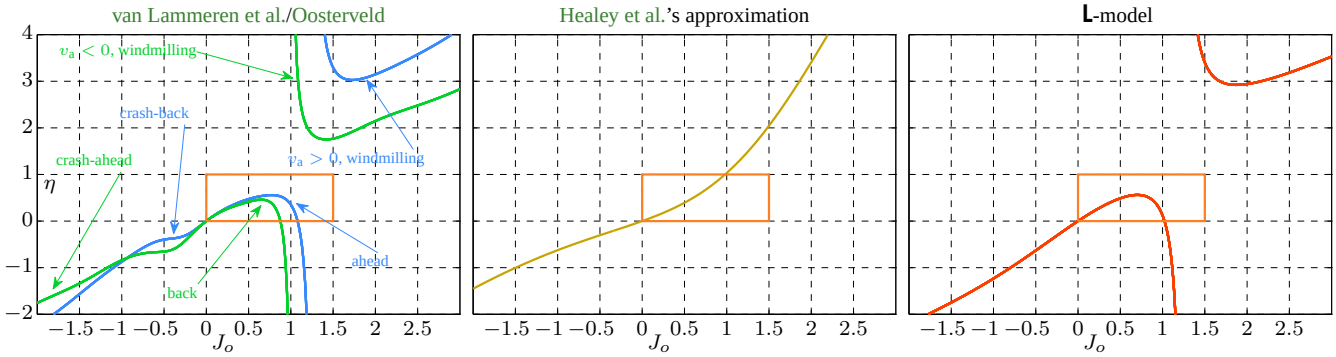

Fig. 5. Comparison of the open-water efficiency $\eta(J_o)$ for the different propeller models, computed for $v_a \in \{-2.0, -1.5, -1.0, -0.5, 0.0, 0.5, 1.0, 1.5, 2.0\}\,\frac{\text{m}}{\text{s}}$ and v_p such that the full range of 360° for β was covered for each value of v_a.

of operation of the propeller. One way to judge the quality of approximation of the **L**-model is to compare its efficiency curve with that corresponding to the **O**-model. For this reason, the efficiency plots for the three models we consider in this paper are presented in Fig. 5. These plots are somehow non-standard, as they depict the efficiency curve over the entire spectrum of possible operating conditions, i.e. over the four possible quadrants of operation. To the best of the authors' knowledge, this kind of "extended" efficiency plot is hardly found in the literature. Indeed, the common practice is to plot the efficiency in just (the part of) the first quadrant where the power used for propulsion, Tv_a, and the power absorbed from the motor, $Q\omega$, are both positive and the propeller is moving ahead, i.e. $v_a > 0$: this corresponds to the blue curve inside the highlighted region of the leftmost plot in Fig. 5. Because each value of J_0 relates to two possible values of the advance angle β (cf. (10)), plotting the efficiency over the four quadrants in terms of the advance ratio J_o requires two curves to cover the entire range of possible propeller operation. For the **O**-model, these are the blue and green curves in the leftmost plot of Fig. 5. Those two curves are identical in case of perfectly symmetric propellers. This holds for the efficiency of the **H**-model and **L**-model depicted in Fig. 5; see also the discussion in Remark 5.

Again, the region usually under consideration for the open-water efficiency (Fossen, 2002, Fig. 12.2) corresponds to the highlighted area in each plot. Since these figures were obtained from four-quadrant models, they are defined even in regions where the original open-water coefficients are not.

4.1 The propeller as a power converter

The shape of η for the **O**-model, as shown in Fig. 5, warrants further explanation. In particular, the presence of the singularity in the efficiency curve can be related to the fact that the propeller should be considered as a non-ideal power converter. The propeller is then viewed as a two-port (static) system that must satisfy the following dissipation inequality (for a thorough discussion about dissipativity, see van der Schaft (2000))

$$Tv_a - Q\omega \leq 0. \tag{14}$$

The intuitive meaning of (14) is that the propeller can only convert (and dissipate) the energy that it receives from the power port (Q, ω) and transmit it to the other power port (T, v_a), and vice-versa.

Using (13), we see that (14) is equivalent to

$$(\eta - 1)Q\omega \leq 0.$$

It follows that, when $Q\omega > 0$, i.e. when the engine is doing work on the propeller, the efficiency η must be smaller than one: this is a familiar bound on the efficiency of a power converter and it simply means that the power available for propulsion is less than the one generated by the motor. When $Q\omega < 0$, however, which is the case when the propeller is used in the windmilling region, then η must be greater than one [3]. The singularity of η occurring at $Q\omega = 0$ allows the efficiency curve to jump from $-\infty$ to $+\infty$ and to satisfy the passivity condition $\eta \leq 1$ for $Q\omega > 0$ and $\eta \geq 1$ for $Q\omega < 0$.

As explained in Sec. 3, the thrust T and torque Q for the **O**-model (as well as for the **L**-model) go to zero for slightly different values of the advance ratio J_0. This do not happen for the **H**-model due to the way the drag and lift coefficients are defined in (8) and (7). Since T and Q are zero for the same value of J_0 in the **H**-model, the corresponding efficiency curve is completely different (and unphysical). The introduction of the two phase-shift coefficients o_{D} and o_{L} and the minimum drag $c_{\text{D}}^{\min}$ in (11) and (12), allows to overcome this simultaneous zero crossing.

4.2 Model Comparison

It is worthwhile considering a comparison of all propeller models mentioned in this work. In van Lammeren et al. (1969), the authors plot the efficiency η against the ratio $k_{\text{T}}/J_{\text{o}}^2$, i.e. related to the first-quadrant model. The equations of the momentum theory and four-quadrant models can be rewritten in such a way that they become compatible with that plot (Oosterveld, 1970, Fig. 31), which is shown next.

Ideal propulsion efficiency. The momentum theory propeller model is an idealized model which can be used to compute the so-called ideal efficiency. Stated simply, the key equations are given in (Sec. 7.3.1 in Clayton and Bishop, 1982, Eq. 7.20 and 7.22), based on the observation that in momentum theory the efficiency is

$$\eta = \frac{P_{\text{out}}}{P_{\text{in}}} = \frac{2}{1 + \left(1 + c_{\text{T}}^{\mathbf{M}}\right)^{1/2}} \quad \text{with} \quad c_{\text{T}}^{\mathbf{M}} := \frac{T}{\frac{1}{2}\rho A v_{\text{a}}^2}$$

where $c_{\text{T}}^{\mathbf{M}}$ is the *momentum theory* thrust coefficient. An in-depth analysis of the assumptions involved is out of the scope of this paper.

Four-quadrant efficiency. Using the relation $k_{\text{T}}/J_{\text{o}}^2 = \frac{\pi}{8} c_{\text{T}}^{\mathbf{M}}$ as e.g. given in (van Lammeren et al., 1969, p. 292), the four-quadrant model can be expressed in a manner that is compatible

[3] In this situation, one would better define the efficiency as $1/\eta = Q\omega/Tv_{\text{a}}$, considering the propeller as a watermill and retrieving the familiar notion of the efficiency being smaller than one. (See also the momentum theory explanation of the windmilling state e.g. in Leishman (2006) for a deeper elaboration.)

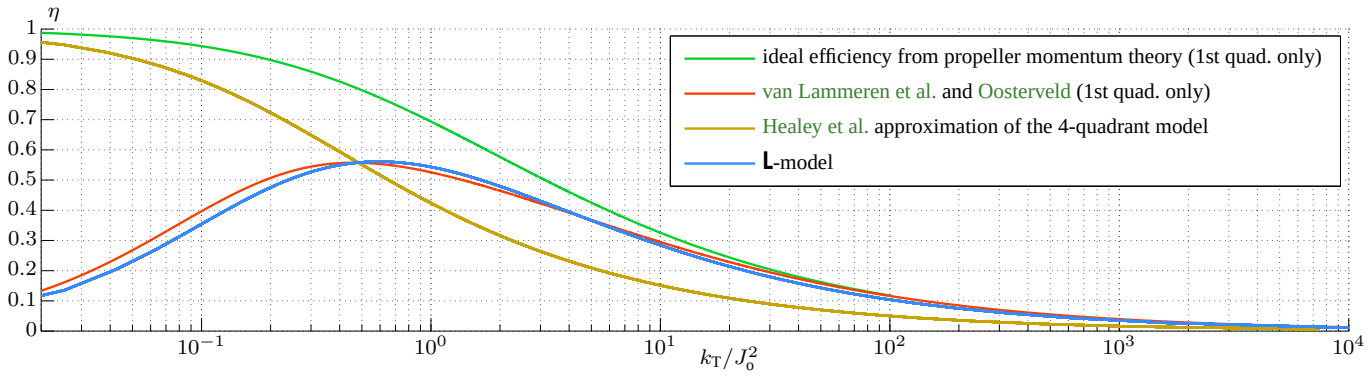

Fig. 6. Open-water efficiency η for all propeller models discussed in this work, inspired by Oosterveld (1970) and van Lammeren et al. (1969).

with the first-quadrant plot of $\eta(k_T/J_o^2)$. To this effect, we note that the open-water efficiency is To thi, we note that the open-water efficiency is

$$\eta = \frac{P_{out}}{P_{in}} = \frac{T v_a}{Q\omega} = \frac{J_o}{2\pi}\frac{k_T}{k_Q} \tag{15}$$

Substituting the conversion equations that are, for instance, given in (Oosterveld, 1970, p. 42) or (Smogeli, 2006, Sec. 2.1.2) into (15), all models can be compared against each other and the ideal efficiency.

Fig. 6 shows clearly how, using the simple **L**-model approximation (motivated by the **H**-model approximation), the propeller efficiency curve of a representative thruster captures the main characteristics of the efficiency curve predicted by the models of van Lammeren et al. (1969) and Oosterveld (1970).

5. CONCLUSION AND PROSPECTIVE WORK

The paper introduced a modified single harmonic approximation to the model of a four-quadrant propeller. The new model builds upon and overcomes some of the difficulties encountered with the model developed by Healey et al.; namely, the fact that the curve of efficiency of a propeller in the first quadrant—derived with this model—does not satisfy first physics principles. The advantages of the new model proposed are threefold: i) it conforms with basic propeller theory, ii) it is simple enough to be used in a more general model of a complete thruster that includes the propeller and the corresponding electrics model, and finally, iii) a comparison of the main propeller characteristics (including the efficiency curve) computed with the suggested model with that obtained with the more complex model by van Lammeren et al. and Oosterveld shows that the key physical properties of the latter are preserved, while achieving a level of smoothness in the curves that appears to be useful in energy optimal trajectory computations.

Future work will include a thorough comparison of the new proposed model with another commonly used model based on momentum theory, as well the study of approximations that reflect non-symmetric propeller behavior.

ACKNOWLEDGEMENTS

The authors expressly thank *Prof. José Alberto C. Falcão de Campos* for a very fruitful discussion of the propeller model introduced in this paper.

REFERENCES

Abbott, I.H.A. and von Doenhoff, A.E. (1959). *Theory of Wing Sections: Including a Summary of Airfoil Data*. Dover Publications, New York, NY, USA.

Anderson, J.D. (1999). *Aircraft Performance and Design*. WCB/McGraw-Hill, Boston, Massachusetts, USA.

Bachmayer, R., Whitcomb, L.L., and Grosenbaugh, M.A. (2000). An Accurate Four-Quadrant Nonlinear Dynamical Model for Marine Thrusters: Theory and Experimental Validation. *IEEE Journal of Oceanic Engineering*, 25(1), 146–159.

Breslin, J.P. and Andersen, P. (1994). *Hydrodynamics of Ship Propellers*, volume 3. Cambridge University Press, Cambridge, UK, and New York, NY, USA, 1st paperback edition.

Carlton, J. (2007). *Marine Propellers and Propulsion*. Butterworth-Heinemann, Oxford, UK, 2nd edition.

Clayton, B.R. and Bishop, R.E.D. (1982). *Mechanics of Marine Vehicles*. Arrowsmith Ltd., Bristol, GB.

Fossen, T.I. (1994). *Guidance and Control of Ocean Vehicles*. Wiley & Sons Ltd., Chichester, GB.

Fossen, T.I. (2002). *Marine Control Systems: Guidance, Navigation, and Control of Ships, Rigs, and Underwater Vehicles*. Marine Cybernetics, Trondheim, Norway.

Glauert, H. (1947). *The Elements of Aerofoil and Airscrew Theory*. Cambridge science classics. Cambridge University Press, Cambridgeshire, UK, and New York, NY, USA, 2nd edition.

Hauser, J. (2002). A Projection Operator Approach to the Optimization of Trajectory Functionals. In *Proceedings of the 15th IFAC World Congress*. Barcelona, Spain.

Häusler, A.J., Saccon, A., Aguiar, A.P., Hauser, J., and Pascoal, A.M. (2012). Cooperative Motion Planning for Multiple Autonomous Marine Vehicles. In *Proceedings of the 9th Conference on Maneuvering and Control of Marine Craft (MCMC)*. Arenzano, Italy.

Häusler, A.J., Saccon, A., Pascoal, A.M., Hauser, J., and Aguiar, A.P. (2013). Cooperative AUV Motion Planning using Terrain Information. In *Proceedings of the OCEANS '13 MTS/IEEE Bergen*. Bergen, Norway.

Healey, A.J., Rock, S.M., Cody, S., Miles, D., and Brown, J.P. (1995). Toward an Improved Understanding of Thruster Dynamics for Underwater Vehicles. *IEEE Journal of Oceanic Engineering*, 20, 354–361.

Leishman, J.G. (2006). *Principles of Helicopter Aerodynamics*. Cambridge University Press, 2nd edition.

Oosterveld, M.W.C. (1970). *Wake Adapted Ducted Propellers*. Ph.D. thesis, Delft University of Technology, Wageningen, The Netherlands.

Pivano, L. (2008). *Thrust Estimation and Control of Marine Propellers in Four-quadrant Operations*. Ph.D. thesis, Norwegian University of Science and Technology (NTNU), Trondheim, Norway.

Sheldal, R.E. and Kilmee, P.C. (1981). *Aerodynamic Characteristics of Seven Symmetrical Airfoil Sections through 180-Degree Angle of Attack for Use in Aerodynamic Analysis of Vertical Axis Wind Turbines*. Technical report, Sandia National Laboratories, Albuquerque, NM, USA.

Smogeli, Ø.N. (2006). *Control of Marine Propellers: From Normal to Extreme Conditions*. Ph.D. thesis, Norwegian University of Science and Technology (NTNU), Trondheim, Norway.

van der Schaft, A.J. (2000). *L_2-Gain and Passivity Techniques in Nonlinear Control*. Communications and Control Engineering Series. Springer, London, UK, and New York, NY, USA.

van Lammeren, W.P.A., van Manen, J.D., and Oosterveld, M.W.C. (1969). The Wageningen B-Screw Series. *Transactions of SNAME*, 77, 269–317.

Whitcomb, L.L. and Yoerger, D.R. (1999). Development, Comparison, and Preliminary Experimental Validation of Nonlinear Dynamic Thruster Models. *IEEE Journal of Oceanic Engineering*, 24(4), 481–494.